

# Adsorptive desulfurization by zinc-impregnated activated carbon: characterization, kinetics, isotherms, and thermodynamic modeling

Sandeep Kumar Thaligari<sup>1</sup> · Vimal Chandra Srivastava<sup>1</sup>  · Basheswar Prasad<sup>1</sup>

Received: 23 August 2015 / Accepted: 30 December 2015 / Published online: 13 January 2016  
© Springer-Verlag Berlin Heidelberg 2016

**Abstract** Sulfur oxides emission because of burning of liquid fuels has become a global environmental challenge. Refineries need to meet ever-stringent liquid fuel standards by using newer desulfurization methods. Present paper reports the results of the studies on adsorptive removal of sulfur compounds from model fuel by zinc-impregnated granular activated carbon (GAC). Zn-loaded adsorbent (Zn-GAC) prepared by wet impregnation method was characterized for its textural, morphological, and structural characteristics by different techniques like liquid nitrogen adsorption, X-ray diffraction (XRD), scanning electron microscopy (SEM), and Fourier transform infrared spectroscopy (FTIR). The adsorbent was further used for the removal of dibenzothiophene (DBT), a sulfur compound, from iso-octane. Equilibrium adsorption was obtained in 6 h. The equilibrium adsorption data were well represented by the Redlich–Peterson isotherm. Thermodynamic parameters were calculated by applying the van't Hoff and Clausius–Clapeyron equations. Values of change in enthalpy and entropy were found to be 4.89 kJ/mol and 30 J/mol K, respectively. Isothermic heat of adsorption was

correlated with surface coverage and heterogeneous nature of the Zn-GAC.

**Keywords** Adsorptive desulfurization · Zinc loaded granular activated carbon · Dibenzothiophene · Adsorption thermodynamics · Isothermic heat of adsorption

## List of symbols

$a_R$	R–P isotherm constant (L/mmol)
$B_1$	Heat of adsorption (kJ/mol)
$C_e$	Liquid phase concentration of the adsorbate at equilibrium (mmol/L)
$h$	Initial adsorption rate (mmol/g min)
$l$	Thickness of the boundary layer (mmol/g)
$k_f$	Pseudo-first-order rate constant ( $\text{min}^{-1}$ )
$k_s$	Pseudo-second-order rate constant (g/mmol·min)
$k_{id}$	Intra-particle diffusion rate constant (mmol/g $\text{min}^{0.5}$ )
$K_F$	Freundlich constant (L/mmol)
$K_L$	Langmuir adsorption constant (L/mmol)
$K_R$	R–P isotherm constant (L/mmol)
$K_T$	Equilibrium binding constant (L/mol)
$q_e$	Uptake of the adsorbate by the adsorbent at equilibrium (mmol/g)
$q_m$	Adsorption capacity of the adsorbent(= $K_R/a_R$ ) (mmol/g)
$R^2$	Coefficient of determination (–)
SSE	Sum of square of error
$T$	Temperature (K)
$\beta$	R–P isotherm constant (–)
$1/n$	Freundlich constant (–)
$\Delta G^\circ$	Gibbs free energy (kJ/mol)
$\Delta H^\circ$	Enthalpy change (kJ/mol)
$\Delta S^\circ$	Entropy change (J/K mol)

**Electronic supplementary material** The online version of this article (doi:10.1007/s10098-015-1090-y) contains supplementary material, which is available to authorized users.

✉ Vimal Chandra Srivastava  
vimalcsr@yahoo.co.in; vimalfch@iitr.ac.in

Sandeep Kumar Thaligari  
sandyout@gmail.com

Basheswar Prasad  
bprasad62@gmail.com

<sup>1</sup> Department of Chemical Engineering, Indian Institute of Technology Roorkee, Roorkee, Uttarakhand 247667, India

## Introduction

For the past few decades, refineries have been forced to produce clean transportation fuels because of the firm environmental regulations on the sulfur and nitrogen emissions. This is due to the presence of sulfur compounds, which are one of the abundant elements in the crude oil (Soleimani et al. 2007). Presence of these compounds in crude has many disadvantages such as poisoning of catalysts during crude oil refining processes, corrosion problems in the pumping, pipeline, refining equipments, and conversion into SO<sub>x</sub> to produce acid rain which damages buildings, automotive paint finishes, acidifies the soils, and severely affects various ecosystems (Srivastava 2012).

To date, most of the refineries rely on the hydrodesulfurization (HDS) method to remove the sulfur compounds, which consumes high energy and requires high temperature (300–450 °C) and high pressure (3–5 MPa) (Whitehurst et al. 1998; Shafi and Hutchings 2000). HDS method facilitates the removal of the aliphatic organosulfur compounds such as thiols, sulfides and disulfides but not the aromatic sulfur compounds such as thiophenes and corresponding derivatives. Using HDS, the octane number of the olefin compounds also gets affected by almost 10 units. Hence, the HDS is expensive and inefficient in removing the ring-structured compounds. Moreover, to achieve the deep desulfurization, HDS requires more high-cost hydrogen, larger reactor volumes, and causes change in the fuel properties. Considering the disadvantages in the HDS method, various other techniques have been developed. Among them, adsorptive desulfurization (ADS) (Jiao et al. 2006; Muzic et al. 2012; Srivastav and Srivastava 2009; Kumar et al. 2011; Yu et al. 2013a; Erdogan et al. 2014) is the one method that can be operated at room temperature and atmospheric pressure. Adsorbents developed should have high selectivity of the ring-structured aromatic compounds which do not get removed by the HDS method, and those adsorbents must be cost effective. Likewise, oxidative desulfurization (ODS) (Kumar et al. 2012; Chen et al. 2013; Tang et al. 2013; Dedual et al. 2014; Mokhtar et al. 2015; Abdullah et al. 2015), can also be performed at room temperature and atmospheric pressure, which is a low cost method. However, ODS method has two shortcomings; firstly, the side reactions produce oxidants which reduce the quality of the fuel. Secondly, the useful olefins get removed by the solvents in the extraction method and the oxidants that have been used are toxic in nature. Another technique of bio-desulfurization (BDS) (Luo et al. 2003; Boniek et al. 2015) in which sulfur compounds from the fuel are removed by using the micro-organisms which decompose the sulfur compounds as energy source. BDS method is advantageous as it is economical and produces

less green house gases. However, slow degradation and challenge of keeping the micro-organisms alive are inherent disadvantages of BDS.

Bio fuels are the alternative fuels that can be produced by various techniques which cause less production of green house gases (Marousek 2013; Marousek et al. 2015) for which subsidy policies have to be formulated and implemented (Marousek et al. 2015).

However, various adsorbents show different capacities of sulfur removal depending on various adsorbent properties. Some studies have been conducted previously for the adsorptive desulfurization by various adsorbents including activated carbon (AC). Zhou et al. (2009) used a batch system in which benzothiophene (BT), dibenzothiophene (DBT), 4,6-dimethyl dibenzothiophene were removed from *n*-octane using active carbon as an adsorbent. Ngamcharussrivichai et al. (2008) used a batch system in which thiophene and BT were removed using zeolites from coal fly ash with *n*-hexane as the model oil. Yu et al. (2013b) carried out batch adsorption studies using hierarchical carbon-encapsulated iron nanoparticles as adsorbent for sulfur removal. Yu et al. (2008) and Gao et al. (2008) studied the role of surface chemistry for sulfur adsorption on carbonaceous materials. Ling et al. (2015) used calcium oxide/carbon foam composites as adsorbents to remove the sulfur in the atmosphere.

In our previous study (Rakesh-Kumar and Srivastava 2012), blank AC was used as an adsorbent for DBT removal from iso-octane. Maximum removal efficiency of 53 % was observed for initial sulfur concentration of 3.125 mmol/L. Central composite (CC) design was employed to optimize the operating conditions; however, kinetic, isotherm, and thermodynamic studies were not reported.

It is known that impregnation of active metal ions can help to increase the adsorptive desulfurization efficiencies and that the literature review shows that zinc-impregnated granular activated carbon (Zn-GAC) has not been used for the ADS. Therefore, in the present study, Zn-GAC has been used for the removal of a sulfur compound, DBT from the model oil (DBT dissolved in iso-octane). Adsorbents, blank-GAC and doped with zinc, have been characterized using various physico-chemical characteristics such as Brunauer–Emmett–Teller (BET) surface area, scanning electron micrograph (SEM), X-ray and energy dispersive diffractogram, fourier transform infrared (FTIR) spectra. The current study also focused on study of the effect of various factors such as initial concentration of DBT ( $C_0$ ), dose of the adsorbent ( $m$ ), and contact time ( $t$ ). Kinetics of the removal process has been studied using various kinetic models. Modeling of equilibrium adsorption data was studied using various isotherm models, and thermodynamic parameters were estimated.

## Materials and methods

### Adsorbent preparation and its characterization

GAC of 8–16 mesh, procured from G.S. Chemical Testing Lab. & Allied Industries, India, was washed with distilled water until it was free from ash. Then it was kept at 100 °C for 6 h for moisture removal. It was further treated with 30 % HNO<sub>3</sub> and was again washed with distilled water unless the pH of the effluent became neutral. After this, it was kept in the oven for 6 h so that the moisture was completely removed. Dried adsorbent and Zn(NO<sub>3</sub>)<sub>2</sub>·6H<sub>2</sub>O (obtained from Himedia Laboratories Pvt Ltd, Mumbai, India) were mixed with sufficient amount of distilled water and subjected to stirring for about 2 h to obtain a 2 % loading. After loading it was again dried, and then calcination was done at 300 °C for 2 h. The calcined adsorbent was then cooled in the desiccator and was used for the removal of DBT. Loading of Zn in the adsorbent was checked by soaking 1 g of catalyst in 10 ml of 65 % nitric acid for 24 h at room temperature so as to dissolve Zn from the adsorbent. The concentration of the Zn in the filtered solution was determined using atomic absorption spectrophotometer (Avanta M by GBC Scientific Equipment Pvt Ltd.). Amount of impregnation was found to vary maximum by ±0.1 times of that intended.

Physico-chemical characterization for the blank-GAC and Zn-GAC was performed using standard procedures. XRD analysis was performed with an X-ray diffractometer (Bruker AXS, Diffractometer D8, and Germany) using Cu-K as source and Ni as filter media. Goniometer speed and the range of the scanning angle ( $2\theta$ ) were 0.5° min<sup>-1</sup> and 5–90°, respectively. The peaks were identified with the ICDD library and their intensity indicated the value of  $2\theta$ , where Bragg's law is applicable. In order to study GAC morphology, scanning electron microscope (SEM) (QUANTA, Model 200 FEG, and USA) was employed. Along with the micrographs, energy dispersive X-ray (EDX) spectra were also taken. Samples were initially gold coated using sputter coater, Edwards S150, in order to provide the conductivity to the samples. Textural characteristic of the adsorbent was studied using a Micromeritics ASAP 2020 apparatus with nitrogen adsorption at 77 K. Surface area of adsorbents was determined by multipoint Brunauer–Emmett–Teller (BET) method. Pore volume and average pore diameter were determined by using Barrett–Joyner–Halenda (BJH) method considering the desorption isotherm. Thermal gravimetric analysis (TGA) and differential thermal analysis (DTA) were carried out in the presence of air in

a temperature range from room temperature up to 1000 °C. The heating rate was kept 10 °C/min.

### Adsorbate

All analytical reagent (AR) grade chemicals were used to perform this study. DBT and iso-octane were obtained from Spectrochem Pvt. Ltd. Mumbai, India and S.D. Fine Chemicals, Mumbai, India, respectively. Stock solution containing 31.25 mmol/L sulfur was prepared by dissolving 0.18 mol of DBT in iso-octane.

### Batch adsorption studies

In every experimental run, 10 mL solution of known sulfur concentration was taken in 25 ml test tube in which pre-measured amount of adsorbent was added. These test tubes were continuously stirred in a temperature-controlled chamber (AQUALYTIC, Germany) maintaining constant stirring rate (500 rpm) and a fixed temperature (30 °C) for all experimental runs. When it comes to isotherm study, different concentrations i.e., 1.56–31.25 mmol/L are taken with the dose 30 g/L and residence time 12 h. The temperature was maintained in the range of 10–40 °C. After predetermined time, the test tubes were removed from the chamber.

### Analysis of DBT

The analysis of DBT was carried out with the help of gas chromatograph (GC) equipped with flame ionization detector (FID) and column 30 m × 0.25 mm Rtx-1 (cross bond 100 % dimethyl poly siloxane), procured from Thermo Fisher Scientific India Pvt Ltd. Nitrogen (N<sub>2</sub>) gas was used as carrier gas. For every GC-FID run, 1 μL volume of the sample was injected and the DBT was identified and analyzed with the standard samples. Prior to the analysis, a calibration plot of known concentrations of DBT (0–15.62 mmol/L) with respect to peak area was made. The sulfur removal percentage and equilibrium adsorption values ( $q_e$  (mmol/g)) were calculated using the following equations:

$$\text{Sulfur removal percentage} = 100(C_o - C_e)/C_o \quad (1)$$

$$\text{Amount of sulfur adsorbed per gram of adsorbent,} \\ q_e = (C_o - C_e)V/m \quad (2)$$

where  $C_o$  is the initial concentration of sulfur (mmol/L),  $C_e$  is the equilibrium sulfur concentration (mmol/L), and  $m$  is the dose of adsorbent (g/L).

## Kinetic study of adsorption

### *Pseudo-first-order and pseudo-second-order model*

Kinetics study was performed for DBT adsorption onto Zn-GAC at different sulfur concentrations of 1.56, 3.125, 7.81, and 15.62 mmol/L. DBT adsorption from the bulk solution onto the surface of Zn-GAC can be considered as a reversible process. Assuming the DBT molecules being adsorbed onto Zn-GAC are non-dissociating and that there is no DBT molecules initially present, the adsorption of DBT onto Zn-GAC at any time ( $q_t$ ) can be represented by the pseudo-first order model (Srivastava et al. 2006) which is given as follows:

$$q_t = q_e[1 - \exp(-k_f t)] \quad (3)$$

where  $q_e$  is the amount of adsorbate adsorbed on the adsorbent at equilibrium and  $k_f$  is the pseudo-first-order rate constant ( $\text{min}^{-1}$ ). The expression for the pseudo-second-order model is as follows (Blanchard et al. 1984; Ho and McKay 1999):

$$q_t = \frac{tk_s q_e^2}{1 + tk_s q_e} \quad (4)$$

The initial adsorption rate,  $h$  ( $\text{mmol/g}\cdot\text{min}$ ), at  $t \rightarrow 0$  is defined as:

$$h = k_s q_e^2 \quad (5)$$

where  $k_s$  is pseudo-second-order rate constant ( $\text{g}/\text{mmol}\cdot\text{min}$ ). The parameters of kinetic models were evaluated by minimizing the sum of square of error (SSE) between the experimental and calculated  $q_t$  values.

### *Diffusion study*

The intra-particle diffusion model is given as (Weber and Morris 1963):

$$q_t = k_{id} t^{1/2} + I \quad (6)$$

where  $k_{id}$  is the intra-particle diffusion rate constant ( $\text{mmol/g}\cdot\text{min}^{0.5}$ ) and value of  $I$  ( $\text{mmol/g}$ ) is the thickness of the boundary layer.

## Results and discussions

### Characterization of blank-GAC and Zn-doped GAC

Average particle size of GAC was 14–16 mesh. The morphologies of blank and Zn-loaded GAC were examined by SEM and XRD analysis. The SEM image of the GAC is shown in Fig. S1 (supporting document). It clearly shows that GAC has considerable number of pores. SEM of doped

GAC shows that the surface texture changed after doping as compared to blank GAC. Figure S1 also shows the dispersion of Zn on GAC which is determined using FE-SEM. It is clearly seen that Zn is well dispersed in the sample. XRD patterns of blank-GAC and Zn-loaded GAC are shown in Fig. S2. XRD spectra of Zn-GAC showed broad peak indicating the presence of amorphous form of silica (Suresh et al. 2011). The broad peak in the XRD indicates amorphous nature of blank- and Zn-GAC. Diffraction peaks corresponding to any crystalline component were not observed in Zn-GAC. This was because of trapping of ZnO inside the crystal lattice of GAC and may be because of amorphous nature of loaded ZnO (Asilturk et al. 2009). Distribution of elements present in blank-GAC and Zn-GAC was checked by EDX analysis. Blank-GAC was found to contain 87.5 % C, 12.4 % O, and 0.45 % Si, whereas Zn-GAC contained 83.7 % C, 13.2 % O, 2.6 % Zn, and 0.4 % Si. Thus, presence of Zn was confirmed by EDX analysis.

BET surface area of blank-GAC and Zn-GAC were found to be 583 and 539  $\text{m}^2/\text{g}$ , respectively. Respective pore volumes were found to be 0.031 and 0.027  $\text{cm}^3/\text{g}$ , whereas BET average pore diameters of blank-GAC and Zn-GAC were found to be 22.94 and 22.92  $\text{\AA}$ , respectively. The analysis of the BJH (Barrett et al. 1951) adsorption pore distribution of the two adsorbents showed that majority of the pore area was only slightly mesoporous ( $20 \text{\AA} < d < 500 \text{\AA}$ ). The decrease in surface area and pore diameter may be due to the adsorption of Zn onto the pore walls of GAC.

TGA analysis was performed to understand the thermal stability of Zn-GAC in the presence of air at the heating rate of 10  $^\circ\text{C}/\text{min}$  (Fig. S3). Up to 400  $^\circ\text{C}$ , there is loss of light volatile molecules and moisture. The weight loss was 17.69 % for Zn-GAC. Higher temperature drying ( $>100 \text{ }^\circ\text{C}$ ) occurs due to loss of the surface tension bound water of the particles. Between room temperature and 400  $^\circ\text{C}$ , Zn-GAC does not show any endothermic transition, indicating no phase changes during the heating process. Zn-GAC showed 77.45 % weight loss between 400  $^\circ\text{C}$  and 625  $^\circ\text{C}$ . The exothermic peak between 400 and 625  $^\circ\text{C}$  represents oxidative degradation of the samples. This study shows that Zn-GAC is fully stable up to 400  $^\circ\text{C}$ .

### Effect of various parameters

The effect of adsorbent dosage ( $m$ ) on the adsorption of DBT onto GAC was studied at  $T = 303 \text{ K}$  and  $C_0 = 15.62 \text{ mmol/L}$  and the results are shown in Fig. S4. It was found that the DBT removal efficiency increased with an increase of dosage from 5 to 30  $\text{g/L}$ . The removal was almost constant for dosage greater than 30  $\text{g/L}$  for Zn-GAC. The increment in the adsorption of DBT with GAC

dose is due to more adsorption sites and higher surface area. At lower dosage, the surface of the GAC becomes saturated with the DBT, leaving no further adsorption. Thus higher the  $m$ , higher is the removal of DBT. However, sulfur adsorbed per gram of adsorbent ( $q$ ) showed maximum value at  $m = 30$  g/L for blank-GAC, whereas it continuously decreased with an increase in  $m$ . Considering the trade-off between the removal efficiency and the  $q$  values, 30 g/L was considered as the optimum adsorbent dose. Earlier, previous studies (Srivastav and Srivastava 2009; Rakesh-Kumar and Srivastava 2012) revealed that the optimum adsorbent dose for DBT removal was 20 g/L.

Sulfur compounds coordinately interact with cations such as  $Zn^{2+}$  with help of lone electron pair of the sulfur atom (Zeng et al. 2008). This enhances the adsorption of the DBT onto Zn-GAC as compared to blank-GAC. FTIR spectra of the Zn-GAC before and after adsorption are shown in the Fig. S5 (supporting information). FTIR of the Zn-GAC before adsorption shows a broadband at  $3132\text{ cm}^{-1}$  which indicates the presence of the free and hydrogen-bonded OH group on the surface of the adsorbent. Peak at  $1750\text{ cm}^{-1}$  indicates the presence of CO group. The band at  $1400\text{ cm}^{-1}$  indicates the presence of the carbonyl group. At around  $1200\text{ cm}^{-1}$ , the spectrum shows transmittance due to stretching of Si–O–Si and C–O–H due to the vibration in lactones and –OH deformation. The peak at around  $605\text{ cm}^{-1}$ , indicates the Si–H bond. It is noticed that the shifting of the peaks takes place after the adsorption due to participation of the functional groups. Thus, along with  $Zn^{2+}$ , various functional groups present on the surface of GAC also help in the adsorption of DBT.

There are some vital factors that restrict the adsorption of the adsorbate molecules onto the adsorbent. These factors include size of adsorbate molecules, adsorbate diffusion coefficient in the bulk and solid phase, the pore size distribution of the adsorbent, adsorbate concentration, and its affinity between the adsorbate and the adsorbent and degree of mixing.

Stock solutions of DBT with varying concentrations  $C_0$  (1.56, 3.12, 7.81, and 15.62 mmol/L) were taken and kept in contact for adsorption till 12 h. Results are shown in Fig. 1. After 6 h of treatment, removal efficiencies of 97.2, 96.1, 79.9, and 74.9 % were observed for  $C_0 = 1.68, 4.04, 8.76,$  and  $17.39$  mmol/L, respectively. Respective values after 12 h of treatment were 98.6, 96.8, 81.4, and 75.8 %. Since the difference in the removal efficiencies values obtained at 6 and 12 h is marginal ( $\pm 2$  % well within the error of the experimental error), quasi-equilibrium can therefore be assumed after 6 h only.

Removal rate of DBT was very rapid initially such that high sulfur removal was obtained in the first 5 min only. Removal rate became gradual after initial fast uptake. In the initial stage of the adsorption, high number surfaces

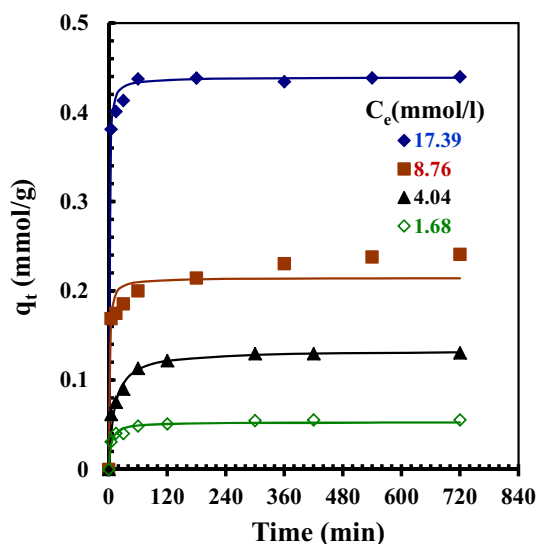


**Fig. 1** Effect of contact time for the removal of sulfur by Zn-GAC. Experimental data points given by the symbols and the lines predicted by the pseudo-second-order model

sites are available for the adsorbate molecules to get adsorbed. As the time increases, the residual adsorbate molecules are repulsed by already adsorbed DBT molecules on the adsorbent phase. In addition to that the DBT molecules should also penetrate deeper to reach the micropores to get adsorbed after being adsorbed into the macro- and meso-pores during the initial phases of adsorption. In order to do so, the molecules experience a great resistance which ultimately reduces the removal rate of DBT.

### Kinetic and diffusion study

For designing the industrial adsorption columns, determination of kinetic and isotherm parameters is necessary. In the current study, adsorption of DBT onto Zn-GAC was evaluated by testing the conventional kinetic models such as pseudo-first-order and pseudo-second-order models. The best-fitted values of  $k_f$ ,  $h$ , and  $k_S$  with coefficient of determination and SSE for the both kinetic models for the adsorption of DBT onto Zn-GAC at the concentrations  $C_0 = 1.56, 3.12, 7.81,$  and  $15.62$  mmol/L at 303 K, are given in Table 1. Also the  $q_{e,exp}$  and the  $q_{e,cal}$  values are shown for the both kinetic models in the Table 1. It may be observed that the  $q_{e,exp}$  and the  $q_{e,cal}$  values almost match each other for the pseudo-second-order kinetic model. Since the coefficient of determination ( $R^2$ ) is nearer to unity for pseudo-second-order as well, the adsorption of the DBT onto Zn-GAC is well explained by the pseudo-second-order kinetic model than pseudo-first-order kinetic model.

The adsorption of the adsorbate molecules from bulk solution to the pores of the adsorbent is generally governed by either one or more steps, e.g., pore diffusion, film

**Table 1** Kinetic parameters for the removal of sulfur by Zn-GAC ( $t = 12$  h,  $C_o = 1.68$ – $17.39$  mmol/L,  $m = 30$  g/L,  $T = 30$  °C)

$C_o$ (mmol/L)	$q_{e,exp}$ (mmol/g)	$q_{e,cal}$ (mmol/g)	$k_f$ (min) <sup>-1</sup>	$R^2$	SSE
Pseudo-first-order model					
1.68	0.05	0.06	0.10	0.724	81.65
4.04	0.13	0.13	0.06	0.883	83.62
8.76	0.24	0.21	0.11	0.689	92.03
17.39	0.44	0.44	0.41	0.695	16.51
$C_o$ (mmol/L)	$q_{e,cal}$ (mmol/g)	$k_s$ (g/mmol min)	$h$ (g/mmol min)	$R^2$	SSE
Pseudo-second-order model					
1.68	0.05	4.06	0.01	0.888	41.57
4.04	0.13	0.64	0.01	0.955	44.54
8.76	0.21	3.44	0.16	0.919	57.32
17.39	0.44	2.98	0.58	0.875	10.21
$C_o$ (mmol/L)	$k_{id,1}$ (mmol/g min <sup>1/2</sup> ) × 10 <sup>-3</sup>	$I_1$ (mmol/g) × 10 <sup>-2</sup>	$R^2$		
W-M-Intra-particle diffusion model					
1.68	2.93	2.58	0.901		
4.04	9.41	3.95	0.997		
8.76	5.76	15.43	0.986		
17.39	10.03	35.97	0.995		
$C_o$ (mmol/L)	$k_{id,2}$ (mmol/g min <sup>1/2</sup> ) × 10 <sup>-3</sup>	$I_2$ (mmol/g) × 10 <sup>-2</sup>	$R^2$		
1.68	0.34	4.70	0.832		
4.04	0.62	11.51	0.779		
8.76	2.00	18.96	0.947		
17.39	0.16	43.45	0.138		

diffusion or external diffusion, and adsorption at the pore surface, or may be the combinations of more than one step. In the process of adsorption, it is essential to find the slowest step. The adsorption process is governed by the external mass transfer for the systems which have poor mixing, small particle sizes of adsorbent, and dilute concentration of adsorbate and higher affinity between the adsorbate and adsorbent. Intra-particle diffusion is applicable for systems which have good mixing, high concentration of adsorbate, and large particle sizes of adsorbent and low affinity of adsorbate for adsorbent (Aravindhan et al. 2007).

If plot of  $q_t$  versus  $t^{0.5}$  follows the linear relationship with the experimental data, then the adsorption process is governed by intra-particle diffusion only, whereas if the experimental data follow the multi-linear relationship, then adsorption process is considered to be influenced by two or more steps. Figure 2 represents a plot of  $q_t$  versus  $t^{0.5}$  plot for DBT adsorption onto Zn-GAC at 303 K. The first sharp portion in the Fig. 2 represents early stage of the adsorption. It indicates that the external mass transfer resistance surrounding the particles is significant, whereas second linear portion shows gradual adsorption with intra-particle diffusion predominating. In Fig. 2, the experimental data

points are elucidated by two straight lines—the first straight line portion indicates the effects of the external mass transfer or boundary layer diffusion (McKay et al. 1980), while the second straight line portion is due to the intra-particle or pore diffusion. Extrapolation to the y-axis, of the straight line sections gives the value of intercept which itself is the boundary layer thickness. The straight line deviation from the origin indicates that the pore diffusion is not the sole rate-controlling step, and this is mainly due to the mass transfer difference in the initial and final stages of adsorption.

The slopes of the plots ( $q_t$  vs.  $t^{0.5}$ ) given by Weber and Morris are explained as a rate parameter, characteristic of the rate of adsorption in intra-particle diffusion region. The values of rate parameters ( $k_{id,1}$  and  $k_{id,2}$ ) are given in Table 1. The values of the correlation coefficients are also given in Table 1.

### Adsorption equilibrium study

The results of the effect of concentration of DBT are shown Fig. 3. It is apparent that the removal of DBT decreases when the concentration of DBT increases, however, the amount of DBT impregnated per unit mass of Zn-GAC

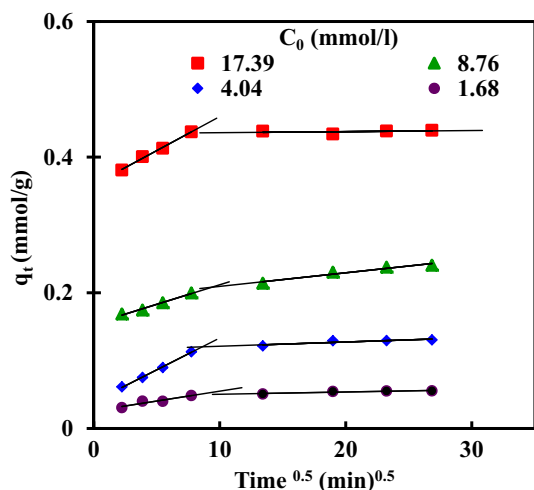


**Fig. 2** Weber and Morris intra-particle diffusion plot for the removal of sulfur by Zn-GAC

increased with an increase in the DBT concentration. This effect is because of the decreased resistance for the adsorption of the DBT from the stock solution.

The adsorption isotherms at various temperatures ranging from 283 K to 313 K,  $q_e$  versus  $C_e$ , are shown in Fig. 4. It is found that the removal of DBT increases with an increase in temperature. At the lower concentrations of adsorbate molecules, the  $q_e$  values increase abruptly but at higher values of adsorbate concentrations the change in  $q_e$  is gradual. Adsorption capacity increased when the temperature was increased because of the endothermic nature of the diffusion process (Rakesh-Kumar and Srivastava 2012). When there is an increase in the temperature, the movement of the adsorbate molecules become faster due to the fact that the diffusing molecules now face less retarding forces. Hence, the adsorption of DBT onto Zn-GAC increased with an increase in temperature.

The isotherm constants for the four isotherms namely Freundlich (1906), Langmuir (1918), Redlich and Peterson (R-P) (1959), and Temkin and Pyzhev (1940) models were studied and the coefficients of determination,  $R^2$ , with the experimental data are reported in Table 2. The  $K_F$  value in the Freundlich isotherm can be taken as a relative indicator of the adsorption capacity of the adsorbent. The magnitude of  $K_F$  shows that the adsorption capacity of Zn-GAC for DBT adsorption increased with an increase in temperature. Values of  $q_m$  for the Langmuir isotherm represent the monolayer saturation at equilibrium, and its value (given in Table 2) increased with an increase in temperature confirming the endothermic nature of overall sorption process for DBT adsorption onto Zn-GAC. Constant  $K_L$  for the Langmuir isotherm corresponds to the concentration at which the amount of DBT bound to the Zn-GAC is equal to  $q_m/2$  and indicates the affinity of the DBT to bind with Zn-GAC. A

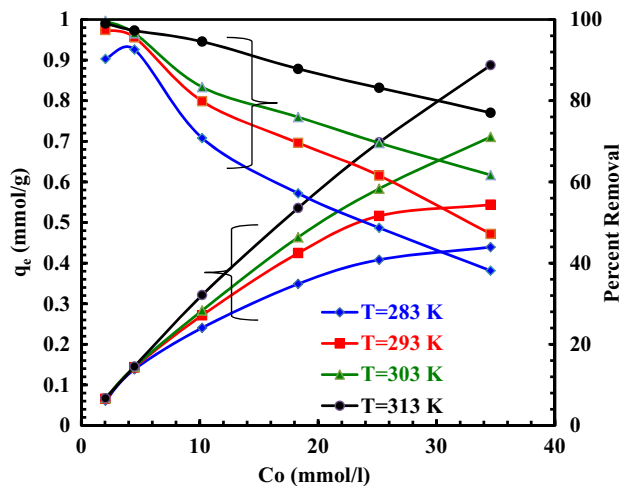


**Fig. 3** Effect of initial sulfur concentration on the removal of sulfur by Zn-GAC

high  $K_L$  value indicates a higher affinity. The R-P isotherm having three constants is applicable for both homogenous and heterogeneous systems. Adsorption process is considered as favorable if the  $\beta$  values lies between 0 and 1. Also if  $\beta = 1$ , R-P isotherm becomes same as Langmuir isotherm and the physio-sorption is the main mechanism of adsorption. Similarly for  $\beta = [1 - (1/n)]$ , the adsorption is more heterogeneous in nature. As per the results given in Table 2,  $\beta$  lies closer to  $[1 - (1/n)]$  as compared to 1, therefore the adsorption of DBT onto Zn-GAC is more heterogeneous in nature. It may be pointed that pseudo-second-order kinetic model which fits the kinetic data is also valid for the heterogeneous nature of the adsorption process.  $R^2$  values for R-P isotherm model are approximately in unity as compared to  $R^2$  values of all other isotherms, and also the SSE error values are least for the fit of R-P isotherm. Hence, R-P model is the best-fit isotherm for the adsorption of the DBT at all the temperatures. The fit of R-P isotherm model on the isotherm data is shown in Fig. 4. The values  $R^2$  and SSE of Freundlich isotherm are also fit to the DBT adsorption but when compared with R-P isotherm,  $R^2$  and SSE values are better for R-P isotherm as compared to other isotherms, hence it the best fit.

**Adsorption thermodynamics**

As per classical thermodynamics, the Gibbs free energy ( $\Delta G_o$ ) is related to enthalpy change ( $\Delta H_o$ ), the entropy change ( $\Delta S_o$ ) at constant temperature ( $T$ ) by the following equation:

$$\Delta G_o = \Delta H_o - T\Delta S_o \tag{7}$$

Using a plot of  $\Delta G_o$  versus  $T$ , the values of the enthalpy and entropy can be evaluated, considering that the  $\Delta H_o$  and  $\Delta S_o$  values remain constant during temperature range

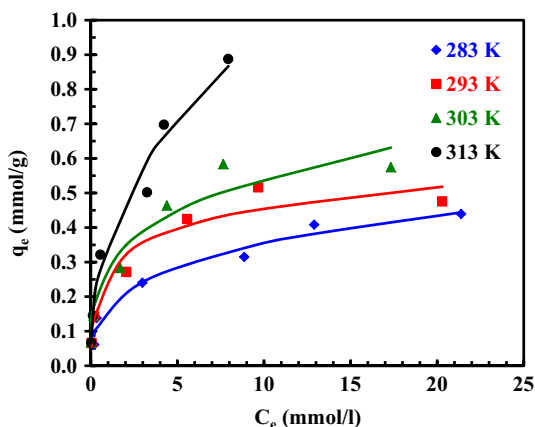


**Fig. 4** Equilibrium adsorption isotherms at different temperatures. Experimental data points given by the symbols and the lines predicted by the R–P model

studied.  $\Delta G_o$  values were found to be  $-4.21$ ,  $4.47$ ,  $-4.90$ , and  $-5.14$  kJ/mol at 283, 293, 303, and 313 K, respectively. The negative sign of the  $\Delta G_o$  implies that the adsorption of DBT onto Zn-GAC is feasible and spontaneous.  $\Delta H_o$  and  $\Delta S_o$  were found to be  $4.89$  kJ/mol and  $0.030$  kJ/mol K, respectively. Also, the positive value of the  $\Delta H^o$  implies that the adsorption process is endothermic in nature. The adsorption of DBT onto Zn-GAC involves mainly two steps: firstly, desorption of the previously adsorbed solvent (iso-octane) molecules, further, adsorption of the adsorbate molecules. More solvent molecules are displaced by the DBT molecules in the DBT-iso-octane system due to which the process needs more energy, resulting in the endothermic nature; ultimately, the value of  $\Delta H^o$  becomes positive. Moreover, due to the enhanced randomness at the interface of the solid and solution with altered structures of adsorbate and adsorbents, the value of  $\Delta S_o$  becomes slightly positive.

Apparent isosteric heat of adsorption ( $\Delta H_{st,a}$ ) at constant surface coverage can be calculated from the slope of the  $\ln C_e$  versus  $(1/T)$  plot using the Clausius–Clapeyron equation (Young and Crowell 1962; Srivastava et al. 2007):

$$\Delta H_{st,a} = R \frac{d \ln C_e}{d(1/T)q_e} \quad (8)$$

$C_e$  at constant amount of DBT adsorbed at different temperatures was calculated using the best-fit equilibrium isotherm model. These isosteres at different  $C_e$  of DBT onto Zn-GAC are shown in Fig. 5. Values of  $\Delta H_{st,a}$  at  $q_e = 0.2, 0.4, 0.6, 0.8,$  and  $1$  mmol/g were found to be  $48.9, 58.8, 64.7, 68.8,$  and  $72.0$  kJ/mol, respectively. The  $\Delta H_{st,a}$  value is low at low coverage and increased steadily with an increase in  $q_e$  indicating that the Zn-GAC has energetically heterogeneous surface.

**Table 2** Isotherm parameters for the removal of sulfur by Zn-GAC ( $t = 12$  h,  $C_o = 1.56$ – $31.25$  mmol/L,  $m = 30$  g/L)

Freundlich $q_e = K_F C_e^{1/n}$					
T (K)	$K_F$ (mmol/g)/(L/mmol) <sup>1/n</sup>	1/n	R <sup>2</sup>	SSE	
283	0.162	0.333	0.985	0.0032	
293	0.238	0.273	0.960	0.0138	
303	0.283	0.280	0.972	0.0136	
313	0.357	0.427	0.988	0.0117	
Langmuir $q_e = \frac{q_m K_L C_e}{1 + K_L C_e}$					
T (K)	$q_m$ (mmol/g)	$K_L$ (L/mmol)	R <sup>2</sup>	SSE	
283	0.435	0.5965	0.960	0.0105	
293	0.522	0.8357	0.973	0.0132	
303	0.654	0.5880	0.982	0.0173	
313	0.962	0.6257	0.967	0.0426	
Temkin $q_e = B_1 \ln K_T + B_1 \ln C_e$					
T (K)	$K_T$ (L/mmol)	$B_1$ (kJ/mol)	R <sup>2</sup>	SSE	
283	13.06	0.074	0.979	0.0046	
293	36.17	0.077	0.971	0.0096	
303	157.9	0.069	0.936	0.0302	
313	41.44	0.128	0.942	0.0574	
Redlich–Peterson $q_e = \frac{K_R C_e}{1 + a_R C_e^b}$					
T (K)	$K_R$ (L/g)	$a_R$ (L/mmol) <sup>1/b</sup>	$\beta$	R <sup>2</sup>	SSE
283	1.69	9.10	0.71	0.987	0.0029
293	1.55	4.88	0.83	0.973	0.0092
303	115.8	405.05	0.72	0.972	0.0136
313	131.2	365.5	0.57	0.988	0.0117

Do and Do (1997) model given by the following equation takes into account both surface heterogeneity as well as the adsorbate–adsorbate interaction:

$$\Delta H_\theta = \Delta H_{o,D} \left\{ 1 - \frac{\alpha \beta \theta}{1 + (\beta - 1)\theta} \right\} + \mu \theta \quad (9)$$

where  $\Delta H_\theta$  is the isosteric enthalpy corresponding to the fractional loading ( $\theta = q/q_m$ ) of DBT, and  $\Delta H_{o,D}$  is the isosteric enthalpy at zero loading calculated using Do and Do model.  $\alpha$  ( $=\delta H/\Delta H_{o,D} < 1$ ) represents the ratio of the variation of the isosteric enthalpy with the fractional loading from zero to monolayer coverage ( $\delta H$ ).  $\beta$  is the pattern parameter representing the pattern of surface heterogeneity and  $\mu$  is the adsorbent–adsorbate interaction energy. The net isosteric heat of adsorption ( $\Delta H_\theta$ ) is obtained after adding the heat of solution ( $\Delta H_{sol}$ ) and the heat of adsorption of iso-octane ( $\Delta H_{iso,o}$ ) to  $\Delta H_{st,a}$ . Because of the non-availability of  $\Delta H_{sol}$  and  $\Delta H_{iso,o}$ , they were



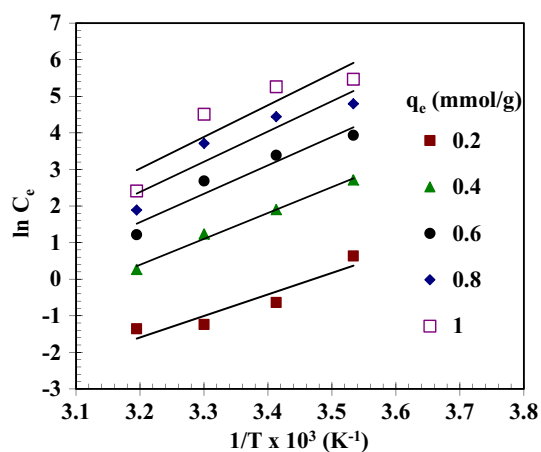


**Fig. 5** Adsorption isosters for determining isosteric heat of adsorption

assumed to be zero and  $\Delta H_\theta$  was considered as  $\Delta H_{st,a}$ . The values of four parameters,  $\Delta H_{o,D}$ ,  $\alpha$ ,  $\beta$ , and  $\mu$ , were estimated by non-linear fitting of the isosteric enthalpy data, and the values were found to be 37.8,  $-6.97$ , 1.1, and  $-230$ , respectively. Thus, considering all factors, DBT adsorption onto Zn-GAC was endothermic in nature.

Spent Zn-GAC was tested after thermal desorption by keeping it first in hot air-oven for 4 h at 373 K and then in the furnace for 6 h at 623 K (Rameshraj et al. 2012). Thermally desorbed Zn-GAC was again used in adsorption experiments in which it showed nearly  $\approx 95\%$  of its capacity that was obtained in the first run. This adsorption–desorption cycle showed that the spent Zn-GAC can be regenerated easily.

## Conclusions

In the present study, Zn-loaded GAC prepared by wet impregnation method was used as adsorbent for the removal of DBT from iso-octane. DBT adsorption process was well elucidated by the multistate diffusion model. DBT uptake was found to be controlled by external mass transfer during early stage of adsorption process and by particle diffusion within the pores of the adsorbent in the later stages. Adsorption kinetics was found to be following pseudo-second-order rate expression. Among all isotherms, R–P isotherm was the best-fitted equilibrium isotherm model at all temperatures. Thermodynamic parameters were calculated by applying the van't Hoff and Clausius–Clapeyron equations. The  $\Delta H_{st,a}$  increased steadily with increase in DBT adsorption onto Zn-GAC indicating heterogeneous Zn-GAC surface. Adsorption process was endothermic in nature. Overall, Zn-GAC can remove DBT (one of the difficult sulfur compound to be removed in the

presently used hydrodesulfurization process) from model liquid fuel and that higher temperature enhanced the desulfurization process.

## References

- Abdullah WNW, Bakar WAWA, Ali R, Embong Z (2015) Oxidative desulfurization of commercial diesel catalyzed by *tert*-butyl hydroperoxide polymolybdate on alumina: optimization by Box–Behnken design. *Clean Technol Environ Policy* 17:433–441
- Aravindhan R, Rao JR, Nair BU (2007) Removal of basic yellow dye from aqueous solution by sorption on green alga *Caulerpa scapelliformis*. *J Hazard Mater* 142:68–76
- Asilturk M, Sayilkan F, Arpac E (2009) Effect of  $Fe^{3+}$  ion doping to  $TiO_2$  on the photocatalytic degradation of malachite green dye under UV and vis-irradiation. *J Photochem Photobiol A* 203:64–71
- Barrett EP, Joyer LG, Halenda PP (1951) The determination of pore volume and area distributions in porous substances: computations from nitrogen isotherms. *J Am Chem Soc* 73:373–380
- Blanchard G, Maunaye M, Martin G (1984) Removal of heavy metals from waters by means of natural zeolites. *Water Res* 18:1501–1507
- Boniek D, Figueiredo D, dos Santos AFB, Stoianoff MAR (2015) Biotransformation: a mini review about the immediate search for the future technology. *Clean Technol Environ Policy* 17:29–37
- Chen Y, Zhang F, Fang Y, Zhu X, Zhen W, Wang R, Ma J (2013) Phosphotungstic acid containing ionic liquid immobilized on magnetic mesoporous silica rod catalyst for the oxidation of dibenzothiophene with  $H_2O_2$ . *Catal Commun* 38:54–58
- Dedual G, MacDonald MJ, Alshareef A, Wu Z, Tsang DCW, Yip ACK (2014) Requirements for effective photocatalytic oxidative desulfurization of a thiophene-containing solution using  $TiO_2$ . *J Environ Chem Eng* 2:1947–1955
- Do DD, Do HD (1997) A new adsorption isotherm for heterogeneous adsorbent based on the isosteric heat as a function of loading. *Chem Eng Sci* 52(2):297–310
- Erdogan S, Koytepe S, Seckin T, Onal Y, Vural S, Basar CA (2014)  $V_2O_5$ –polyimide hybrid material: synthesis characterization and sulfur removal properties in fuels. *Clean Technol Environ Policy* 16:619–628
- Freundlich HMF (1906) Over the adsorption in solution. *J Phys Chem* 57:385–471
- Gao ZM, Bandosz TJ, Zhao ZB, Han M, Liang CH, Qiu JS (2008) Investigation of the role of surface chemistry and accessibility of cadmium adsorption sites on open-surface carbonaceous materials. *Langmuir* 24:11701–11710
- Ho YS, McKay G (1999) Pseudo-second order model for sorption processes. *Process Biochem* 34:451–465
- Jiao H-Y, Yang L-N, Shen J, Li J, Qi Y-T (2006) Desulfurization of FCC gasoline over mordenite modified with  $Al_2O_3$ . *Pet. Sci Technol* 24:1301–1306
- Kumar S, Srivastava VC, Badoni RP (2011) Studies on adsorptive desulfurization by zirconia based adsorbents. *Fuel* 90:3209–3216
- Kumar S, Srivastava VC, Badoni RP (2012) Oxidative desulfurization by chromium promoted sulfated zirconia. *Fuel Process Technol* 93:18–25
- Langmuir I (1918) The adsorption of gases on plane surfaces of glass mica and platinum. *J Am Chem Soc* 40:1361–1403
- Ling Z, Wan P, Yu C, Xiao N, Yang JY, Long Y, Qiu JS (2015) One-pot fabrication of calcium oxide/carbon foam composites for the adsorption of trace  $SO_2$ . *Chem Eng J* 259:894–899

- Luo MF, Xing JM, Liu HZ (2003) Desulfurization of dibenzothiophene by lyophilized cells of *Pseudomonas delafieldii* R-8 in the presence of dodecane. *Biochem Eng J* 13:1–6
- Marousek J (2013) Use of continuous pressure shockwaves apparatus in rapeseed oil processing. *Clean Technol Environ Policy* 15:721–725
- Marousek J, Haskova S, Zeman R, Vachal J, Vanickova R (2015) Assessing the implications of EU subsidy policy on renewable energy in Czech Republic. *Clean Technol Environ Policy* 17:549–554
- McKay G, Otterburn MS, Sweeney AG (1980) The removal of color from effluent using various adsorbents. III Silica: rate processes. *Water Res* 14:15–20
- Mokhtar WNAW, Bakar WA, Ali R, Kadir AA (2015) Catalytic oxidative desulfurization of diesel oil by Co/Mn/Al<sub>2</sub>O<sub>3</sub> catalysts—tert-butyl hydroperoxide (TBHP) system: preparation, characterization, reaction, and mechanism. *Clean Techn Environ Policy* 17:1487–1497
- Muzic M, Katica Sertic-Bionda K, Adzamic T (2012) Evaluation of commercial adsorbents and their application for desulfurization of model fuel. *Clean Techn Environ Policy* 14:283–290
- Ngamcharussrivichai C, Chatratananon C, Nuntang S, Prasassarakich P (2008) Adsorptive removal of thiophene and benzothiophene over zeolites from mae moh coal fly ash. *Fuel* 87:2347–2351
- Rakesh-Kumar D, Srivastava VC (2012) Studies on adsorptive desulfurization by activated carbon. *Clean-Soil Air Water* 40:545–550
- Rameshraj D, Srivastava VC, Kushwaha JP, Mall ID (2012) Quinoline adsorption onto granular activated carbon and bagasse fly ash. *Chem Eng J* 181–182:343–351
- Redlich O, Peterson DL (1959) A useful adsorption isotherm. *J Phys Chem* 63:1024
- Shafi R, Hutchings GJ (2000) Hydrodesulfurization of hindered dibenzothiophenes: an overview. *Catal Today* 59:423–442
- Soleimani M, Bassi A, Margaritis A (2007) Biodesulfurization of refractory organic sulfur compounds in fossil fuels. *Biotechnol Adv* 25:570–596
- Srivastav A, Srivastava VC (2009) Adsorptive desulfurization by activated alumina. *J Hazard Mater* 170:1133–1140
- Srivastava VC (2012) An evaluation of desulfurization technologies for sulfur removal from liquid fuels. *RSC Adv* 2:759–783
- Srivastava VC, Swamy MM, Mall ID, Prasad B, Mishra IM (2006) Adsorptive removal of phenol by bagasse fly ash and activated carbon: equilibrium kinetics and thermodynamics. *Colloids Surf A* 272:89–104
- Srivastava VC, Mall ID, Mishra IM (2007) Adsorption thermodynamics and isosteric heat of adsorption of toxic metal ions onto bagasse fly ash (BFA) and rice husk ash (RHA). *Chem Eng J* 132(1–3):267–278
- Suresh S, Srivastava VC, Mishra IM (2011) Study of catechol and resorcinol adsorption mechanism through granular activated carbon characterization, pH and kinetic study. *Sep Sci Technol* 46(11):1750–1766
- Tang Q, Lin S, Chenq Y, Liu S, Xiong JR (2013) Ultrasound-assisted oxidative desulfurization of bunker-C oil using tert-butyl hydroperoxide. *Ultrason Sonochem* 20:1168–1175
- Tempkin MJ, Pyzhev V (1940) Heavy metals removal and isotherms study. *Acta Physiochim URSS* 12:217–222
- Weber WJ Jr, Morris JC (1963) Kinetics of adsorption on carbon from solution. *J Sanit Eng Div* 89:31–59
- Whitehurst DD, Isoda T, Mochida I (1998) Present state of the art and future challenges in the hydrodesulphurization of poly aromatic sulfur compounds. *Adv Catal* 42:345–471
- Young DM, Crowell AD (1962) *Physical adsorption of gases*. Butterworths, London
- Yu C, Qiu JS, Sun YF, Li XH, Chen G (2008) Adsorption removal of thiophene and dibenzothiophene from oils with activated carbon as adsorbent: effect of surface chemistry. *J Porous Mater* 15:151–157
- Yu C, Fan X, Yu L, Bandosz TJ, Zho Z, Qiu J (2013a) Adsorptive removal of thiophenic compounds from oils by activated carbon modified with concentrated nitric acid. *Energy Fuels* 27:1499–1505
- Yu C, Sun YF, Fan XM, Zhao ZB, Qiu JS (2013b) Hierarchical carbon-encapsulated iron nanoparticles as a magnetically separable adsorbent for removing thiophene in liquid fuel. *Part Part Syst Char* 30:637–644
- Zeng Y-P, Ju S, Xing WH, Chen CL (2008) Adsorption of mercaptan from model gasoline on 13X loaded with Zn<sup>+2</sup>. *Can J Chem Eng* 86:186–191
- Zhou H, Li G, Wang X, Jin C, Chen Y (2009) Preparation of a kind of mesoporous carbon and its performance in adsorptive desulfurization. *J Nat Gas Chem* 18:365–368